

ORIGINAL ARTICLE

Neural correlates of value-driven spatial orienting

Ming-Ray Liao  | Andy J. Kim | Brian A. Anderson

Department of Psychological and Brain Sciences, Texas A&M University, College Station, Texas, USA

Correspondence

Ming-Ray Liao, Department of Psychological & Brain Sciences, Texas A&M University, 4235 TAMU, College Station, TX 77843-4235, USA.
Email: m4liao@tamu.edu

Funding information

Brain & Behavior Research Foundation, Grant/Award Number: NARSAD 26008; National Institute on Drug Abuse, Grant/Award Number: R01-DA406410

Abstract

Reward learning has been shown to habitually guide overt spatial attention to specific regions of a scene. However, the neural mechanisms that support this bias are unknown. In the present study, participants learned to orient themselves to a particular quadrant of a scene (a high-value quadrant) to maximize monetary gains. This learning was scene-specific, with the high-value quadrant varying across different scenes. During a subsequent test phase, participants were faster at identifying a target if it appeared in the high-value quadrant (valid), and initial saccades were more likely to be made to the high-value quadrant. fMRI analyses during the test phase revealed learning-dependent priority signals in the caudate tail, superior colliculus, frontal eye field, anterior cingulate cortex, and insula, paralleling findings concerning feature-based, value-driven attention. In addition, ventral regions typically associated with scene selection and spatial information processing, including the hippocampus, parahippocampal gyrus, and temporo-occipital cortex, were also implicated. Taken together, our findings offer new insights into the neural architecture subserving value-driven attention, both extending our understanding of nodes in the attention network previously implicated in feature-based, value-driven attention and identifying a ventral network of brain regions implicated in reward's influence on scene-dependent spatial orienting.

KEYWORDS

eye movements, fMRI, learning, reward, spatial orienting

1 | INTRODUCTION

Selectively representing relevant and important information is necessary for us to effectively navigate dense visual environments. Our brains must accordingly facilitate this process, and much evidence suggests that our perceptual experience is the product of a competitive process in which attention biases perception in favor of selected stimuli (Desimone & Duncan, 1995). Sources of

attentional bias include top-down factors such as task goals (Folk et al., 1992; Wolfe et al., 1989), bottom-up factors such as physical salience (Theeuwes, 1992), and selection history from associative reward learning (Anderson, 2016; Anderson et al., 2011; Hickey et al., 2010), statistical regularities (Britton & Anderson, 2020; Wang & Theeuwes, 2018a, 2018b, 2018c), and aversive conditioning (Anderson & Britton, 2019; Nissens et al., 2017; Schmidt et al., 2015).

This is an open access article under the terms of the [Creative Commons Attribution](https://creativecommons.org/licenses/by/4.0/) License, which permits use, distribution and reproduction in any medium, provided the original work is properly cited.

© 2023 The Authors. *Psychophysiology* published by Wiley Periodicals LLC on behalf of Society for Psychophysiological Research.

The role of associative reward learning in guiding feature-based attention is well established (see Anderson et al., 2016, for a review). Numerous studies have demonstrated that previously rewarding stimuli continue to bias attention into extinction (Anderson & Yantis, 2013; Liao & Anderson, 2020a; Milner et al., 2023), even when the reward-associated feature is nonsalient, no longer task-relevant, and no longer predictive of reward. The features commonly employed include but are not limited to colors (Anderson et al., 2011; Le Pelley et al., 2015), shapes (Della Libera et al., 2011; Della Libera & Chelazzi, 2009), orientations (Laurent et al., 2015), and object categories (Donohue et al., 2016; Hickey et al., 2015). The neural correlates of value-driven attention for features are also well established and include the ventral visual cortex, frontal eye field, and caudate tail (Anderson et al., 2014, 2016; Barbaro et al., 2017; Donohue et al., 2016; Hickey & Peelen, 2015, 2017; Ikeda & Hikosaka, 2003; Kim & Anderson, 2020a, 2020b; Kim & Hikosaka, 2013; Yamamoto et al., 2013; see Anderson, 2019 for a review). The early visual cortex (Itthipuripat et al., 2019; MacLean & Giesbrecht, 2015; Serences, 2008; Serences & Saproo, 2010) and insula (Wang et al., 2015) have also been implicated.

More recently, some studies have demonstrated that reward learning can also guide overt spatial attention, or spatial orienting (Anderson & Kim, 2018a, 2018b; Chelazzi et al., 2014; see also Liao & Anderson, 2020b). In Anderson and Kim (2018a), participants learned to associate a region in space within distinctive object-rich scenes with reward. After this learning, they performed a visual search task superimposed on the scenes. It was found that target identification was facilitated when the target appeared in the previously reward-associated region (valid trial). Eye movements were likewise biased toward the previously reward-associated region (Anderson & Kim, 2018a, 2018b).

Evidence from both behavior (e.g., Anderson & Kim, 2019a, 2019b; Anderson & Yantis, 2012; Kim & Anderson, 2019a) and neuroimaging (e.g., Anderson, 2017, 2019; Anderson et al., 2014, 2016; Kim & Anderson, 2020a, 2020b) in the case of value-driven feature-based attention and behavior in the case of value-driven spatial orienting (Anderson & Kim, 2018a, 2018b; Liao & Anderson, 2020b) suggest a common influence on the oculomotor system. This opens up the possibility of a common network of brain regions subserving both modes of value-modulated orienting. This includes the caudate tail, which is causally linked to eye movements (Yamamoto et al., 2012), along with the superior colliculus (to which the caudate tail projects via the substantia nigra pars reticulata; Yamamoto et al., 2012) and frontal eye field (to which the superior colliculus projects via the mediodorsal thalamus; Sommer & Wurtz, 2004). A recent study investigating

value-driven attentional capture following exogenous spatial cues confirmed that the frontal eye field, parietal cortex, superior colliculus, and striatum were involved in both goal-directed and reward-related shifts of attention (Bourgeois et al., 2022). Although this study used simple objects (circles and diamonds) and the spatial element was in the form of an exogenous cue that was not related to the reward-associated feature (color), there is converging evidence for a system underlying value-driven attentional orienting that integrates sources of feature- and space-based guidance.

A unique element of value-driven spatial orienting is the reliance on object-rich scenes that can provide contextual information about where to guide overt attention (Brockmole & Henderson, 2006a, 2006b). With the inclusion of complex objects and spatial layout that collectively serve as a cue for a high-value region, we expect parts of the medial temporal lobe like the hippocampus and parahippocampal gyrus—not previously implicated in value-driven feature-based attention (see Anderson, 2019)—to play an important role in signaling scene-specific spatial biases. The caudate tail receives input via the ventral visual stream and in particular the visual cortico-striatal loop (Anderson, 2019; Seger, 2013); the ventral visual cortex is robustly activated by complex scenes in a manner modulated by reward (Barbaro et al., 2017; Hickey & Peelen, 2015, 2017), and the caudate tail runs adjacent to the hippocampus and surrounding parahippocampal gyrus, which play a well-defined role in spatial memory (Epstein & Kanwisher, 1998; Maguire et al., 1996; O'Keefe & Nadel, 1978). Value-driven attention for low-level features is sensitive to specific scene contexts (Anderson, 2015; see also Grégoire et al., 2021) which, along with the caudate tail's proximity to the medial temporal lobe (Seger, 2013) and its connections with the superior colliculus (Ikeda & Hikosaka, 2003; Yamamoto et al., 2012), raise the possibility that this network of brain regions is collectively involved in representing value-driven spatial orienting.

Using human functional magnetic resonance imaging (fMRI), we employed a whole-brain approach to investigate the representation of task-irrelevant, value-driven spatial orienting biases using the paradigm established by Anderson and Kim (2018a). In this task, valid trials necessitate an eye movement to the region of a scene previously associated with high value, while on invalid trials we would expect less robust processing of the previously reward-associated region. Given the aforementioned considerations, we hypothesized that, when controlling for the position of the target, valid trials would be associated with more robust activation (biased competition driven by the reward history of the target quadrant) in oculomotor regions of the brain previously implicated in value-driven feature-based attention (caudate tail, superior colliculus,

frontal eye field) in addition to the hippocampus and parahippocampal gyrus given the reliance on scene context. It is important to note that our paradigm focuses on spatial biases as measured by overt attentional orienting, which may yield different findings compared to covert spatial attention (Hunt & Kingstone, 2003a, 2003b).

2 | METHOD

2.1 | Participants

Forty-seven participants (18–35 years of age, $M=22.83$ years, $SD=4.55$; 24 females, 23 males) were recruited from the Texas A&M Community. The demographic information for one participant was lost due to experimenter error. Participants were compensated with money earned from the experimental task. All reported normal or corrected-to-normal visual acuity and normal color vision. All procedures were approved by the Texas A&M University Institutional Review Board and conformed with the principles outlined in the Declaration of Helsinki. All participants provided written informed consent. Of the 47 recruited participants, eight did not meet the required task performance to continue in the scanner (failed to robustly learn the pairings between locations in scenes and rewards or could not perform that test phase task with sufficient accuracy; additional details are provided later in the Methods section), and five withdrew partway through the study. The final sample consisted of 34 participants who completed the entire experiment, for which 33 of their demographic data is available ($M=22.33$ years, $SD=4.36$; 15 females, 18 males). The obtained sample size provided power $(1-\beta) > 0.9$ to replicate an effect of reward learning on eye movements in the test phase of Anderson

and Kim (2018a, 2018b) (computed using G*Power 3.1), and was similar to (and in most cases exceeded) the sample sizes used in prior studies of the neural correlates of value-driven attention (Anderson, 2017; Anderson et al., 2014; Barbaro et al., 2017; Hickey & Peelen, 2015; Itthipuripat et al., 2019; Kim & Anderson, 2019b, 2019c, 2020a, 2020b).

2.2 | Apparatus

In-lab tasks were completed on a Dell OptiPlex equipped with Matlab software and Psychophysics Toolbox extensions (Brainard, 1997). Stimuli were presented on a Dell P2717H monitor. Participants viewed the monitor from a distance of approximately 70 cm in a dimly lit room. Manual responses were entered using a standard keyboard. Eye tracking was conducted using the EyeLink 1000 Plus system, while head position was maintained using a manufacturer-provided chin rest (SR Research Ltd.). Stimulus presentation during the fMRI portion was controlled by an InVivo SensaVue display system. The eye-to-screen distance was approximately 125 cm. Responses were entered using Cedrus Lumina two-button response pads. An EyeLink 1000 Plus system was again used to track eye position.

2.3 | Training phase

Each trial began with a fixation cross (1.1° visual angle) that remained at the center of the screen until eye position had been registered within 1.8° of the fixation cross for a continuous period of 500 ms (Figure 1). After which, a scene image was displayed that filled the entire computer screen. Four gray rectangular outlines (9.1°

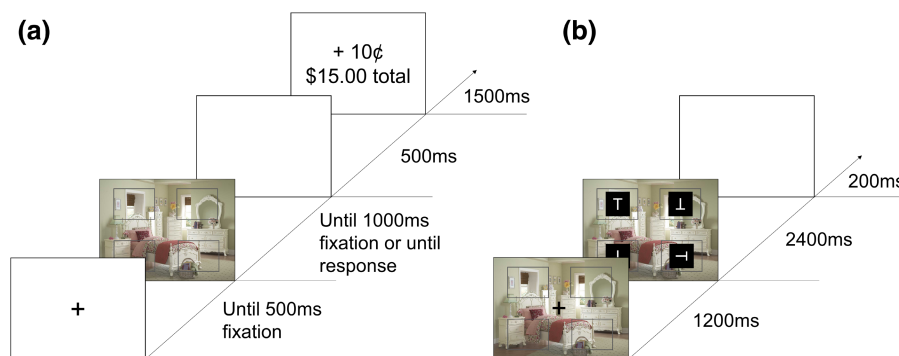


FIGURE 1 Time course of trial events during the training and test phases of the experiment. During the training phase, (a) participants were presented with scenes with an empty box in each quadrant and instructed to pick a box by looking directly at it. Depending on their choice, participants earn either 10c or 2c on every trial. During the test phase (b) participants were tasked with searching for a side ways “T” among upright and upside down “T” distractors. Scenes previously experienced during the training phase were used as background and were irrelevant to the task. Note that the stimuli are not drawn to scale in the figure, and the background has been changed from black to white for display purposes.

$\times 6.9^\circ$) were also displayed at the center of each quadrant, the center of which was 11.4° away from the center of the screen. The scene and rectangles remained on the screen until the eye position had been registered within the boundary of one of the rectangles for a continuous period of 1000 ms. After a 500-ms blank screen, the reward feedback display was presented for 1500 ms and consisted of the money earned on the current trial along with the updated total earnings.

Participants were instructed to fixate (“look directly at”) the cross to begin each trial, then to “pick a box and look directly at it.” Participants were also informed that they would earn money on each trial, and the amount earned would depend on which box they looked in. Participants were encouraged to maximize their earnings by picking good boxes but were otherwise not provided any explicit information about which boxes were good. There were four 80-trial runs of the training phase during the in-lab visit, and two runs of abridged training phases that only had 40 trials while in the scanner. There were eight practice trials before the in-lab training phases, where participants earned 5¢ on each trial but were informed that the money earned was for demonstration purposes only. Eight different scenes were used in the experiment, totaling 50 presentations of each scene over 400 trials. The scenes were taken from the CB Database (Sareen et al., 2016) and were used in previous studies of value-driven spatial orienting (Anderson & Kim, 2018a, 2018b). For each scene, one quadrant (and the box it contained) was designated the high-value quadrant and yielded a 10¢ reward, while picking any other boxes yielded a 2¢ reward.

Participants were assigned to one of four training conditions in alternating fashion, with each quadrant of each scene serving as the high-value quadrant in one of the four conditions. The order in which the scenes were presented to each participant was randomized. If eye tracking was unable to be conducted in the scanner, participants instead used two two-button response pads to indicate their selection on each trial (one button per quadrant) and received some initial practice trials to learn the button mapping. To be eligible for the scanning session, participants needed to earn at least \$4.00 during the last training phase run conducted in the lab, which was taken to indicate sufficiently robust learning of the scene-reward contingencies (Figure S1).

2.4 | Test phase

Each trial began with the presentation of one of the scenes from training along with the 4 rectangular boxes for 1200 ms, followed by the presentation of a 1.1° “T”

stimulus in white against a black background centered within each of the boxes. One “T” was tilted either 90° to the left or right and served as the target, while the other three “T”s were either upright or upside down (randomly determined with the constraint that all three nontarget “T”s could not be oriented in the same direction). The display remained on screen for 2400 ms, during which participants could enter their responses. That is, the duration of the display was fixed for all participants regardless of response time (RT). For a subset of participants, eye-tracking data were also collected during this time, and eye positions within a region extending $4.6^\circ \times 3.4^\circ$ beyond the boundary of the rectangle for a continuous period of 100 ms were counted as fixations. Unlike the training phase, eye movements in the test phase were neither encouraged nor discouraged, although the size and position of the “T” stimuli were such that the identity of the target would be very difficult to resolve using the peripheral vision. Each trial ended with a blank inter-trial interval (ITI), which lasted 1200, 1800, 2400, 3000, or 3600 ms (equally often). The fixation cross reappeared for the last 200 ms of the ITI to indicate to the participant that the next trial was about to begin. The test phase consisted of six runs of 80 trials each for a total of 480 trials, with each scene being presented a total of 60 times. During each run, there were 16 trials where the “T” displays never appeared and the scene continued to stay on the screen for 2400 ms (nonsearch trials). During the 64 search trials (containing the “T” display) in each run, the target appeared in each box or quadrant of each scene equally often (and thus the target position was unbiased with respect to which quadrant previously served as the high-value quadrant). The target was tilted 90° to the left and right equally often for each scene. Trials were presented in a random order. At the end of each run, the accuracy of the 64 target trials was displayed for six seconds to provide performance feedback.

During the in-lab visit, participants were instructed to press the “m” key with their right-hand index finger if the vertical line of the sideways “T” was on the left, denoting an arrow pointing to the right. If the vertical line of the sideways “T” was on the right, participants were instructed to press the “z” key with their left-hand index finger. To become familiar with the mapping, participants had 8 practice trials that included feedback displays that said “Correct!” or “Incorrect!” depending on their response, after which participants had four runs of 80 trials to reach 85% accuracy and be eligible for scanning. If participants reached 85% accuracy in one of these runs, they became eligible and moved on to the next task. During the scan-center visit, participants were instructed to indicate the orientation of the target with

their right-hand index and middle fingers on the button response pad (Table S1).

2.5 | Procedure

The experiment consisted of a lab visit for 1 hr followed by a scan-center visit on the following day. During the initial appointment, participants provided their consent, completed the MRI safety screening, and were screened for adequate performance on the behavioral task. The majority of scene-reward training took place during the lab visit. Each eligible participant underwent fMRI in a single 1.25-hr session that took place the following day. Participants completed one run of the training phase, three runs of the test phase, an anatomical scan, another run of the training phase, and lastly completed three more runs of the test phase. The abridged training phases were completed to re-instantiate the space-outcome associations to protect against possible extinction (e.g., Lee & Shomstein, 2014).

2.6 | Measurement of eye position

During the lab visit, head position was maintained using an adjustable chin rest, including a bar upon which to rest the forehead (SR Research). Participants were given a short break between different runs of the task, during which they were allowed to reposition their heads to maintain comfort. During the fMRI scan, head position was restricted using foam padding within the head coil, and eye tracking was conducted using the reflection of the participant's face on the mirror attached to the head coil. Participants were given short breaks in between runs where they were allowed to close their eyes but otherwise were encouraged to remain still. Eye position was calibrated prior to each run of trials using a 9-point calibration (Liao & Anderson, 2020a, 2020b; Liao et al., 2020) and was manually drift-corrected by the experimenter during the initial fixation display as necessary. Due to the difficulty of measuring eye position in the scanner environment, eye data could only be acquired for a subset of participants ($n = 19$) during the scan session.

2.7 | MRI data acquisition

MRI data were acquired with a Siemens 3-Tesla MAGNETOM Verio scanner and a 32-channel head coil at the Texas A&M Translational Imaging Center (TIC), College Station, TX. An anatomical scan was acquired using a T1-weighted magnetization prepared rapid gradient echo (MPRAGE) sequence (150 coronal slices, voxel

size = 1 mm isotropic, repetition time (TR) = 7.9 ms, echo time (TE) = 3.65 ms, flip angle = 8°. Whole-brain functional images were acquired using a T2*-weighted echo planar imaging (EPI) sequence (56 axial slices, TR = 600 ms, TE = 29 ms, flip angle = 52°, image matrix = 96 × 96, field of view = 240 mm, slice thickness = 2.5 mm with no gap), using the same parameters as Kim and Anderson (2019c, 2020a, 2020b). Each EPI pulse sequence began with dummy pulses to allow the MR signal to reach steady state and concluded with an additional 6 sec blank epoch. Each of the 6 runs of the test phase lasted 8.1 mins during which 810 volumes were acquired.

2.8 | Behavioral data analyses

In the training phase, performance was categorized in terms of how many times the high-value quadrant was chosen per run, averaged over the scenes. A one-way analysis of variance (ANOVA) was conducted on the proportion of high-value choices for each run, followed by a pair-wise comparison between the first and last runs of the training phase. Only training phase data collected in the lab were analyzed. In the test phase, RT was recorded from the onset of the four items comprising the search array, and RTs exceeding 2.5 *SD* of the mean of their respective conditions or faster than 150 ms were trimmed (2.78%). If eye-tracking data were available, the proportion of first saccade toward the high-value quadrant was compared to chance (25%); in addition, on no-target trials (which amounted to a free-viewing situation), total fixation duration was also computed for each quadrant, and the mean for the high-value quadrant was compared to the mean of a given low-value quadrant (mean across low-value quadrants divided by three, paralleling Anderson & Kim, 2018a, 2018b). Only the correct responses were analyzed. The effect sizes *d* were also computed, but the data were not otherwise transformed. Data were analyzed using SPSS and MATLAB, and figures were generated in Python using the Seaborn package (Waskom, 2021).

2.9 | MRI data analyses

2.9.1 | Preprocessing

All preprocessing was conducted using the AFNI software package (Cox, 1996). Each EPI run for each participant was motion corrected using the last image prior to the anatomical scan as a reference. EPI images were then coregistered with the corresponding anatomical image for each participant. The images were then nonlinearly warped to the Talairach brain (Talairach & Tournoux, 1988) using

3dQwarp, and masks of activation locations were created for each participant using 3dAutoMask and combined using 3dmask_tool. Additionally, the cerebrospinal fluid mask was generated using 3dSeg and subtracted from the combined mask for all participants. Finally, the EPI images were converted to percent signal change normalized to the mean of each run and then spatially smoothed to a resulting 5 mm full-width half-maximum using 3dBlurToFWHM.

2.9.2 | Statistical analyses

All statistical analyses were performed using the AFNI software package. A general linear model (GLM) was performed on the test phase data and included the following regressors of interest: (1) valid trial, where the target appeared in the previously high-value quadrant in the left visual field, (2) valid trial, reward/target location in the right visual field, (3) invalid trial, both reward and target location in the left visual field (same hemifield but in different quadrants), (4) invalid trial, both reward and target location in the right visual field, (5) invalid trial, target location in the left visual field and reward location in the right visual field, (6) invalid trial, target location in the right visual field and reward location in the left visual field, and no-target trials with (7) reward location in the left visual field and (8) reward location in the right visual field. Each regressor of interest was modeled using sixteen finite impulse response functions (e.g., Kim & Anderson, 2019c, 2020a, 2020b) beginning at the onset of stimulus presentation, and drift in the scanner signal was modeled using nuisance regressors.

To compare the peak of the hemodynamic response, the peak β value from the 3–6 s range (i.e., 3, 3.6, 4.2, ... 6) post scene display onset for each task-based regressor was extracted (Kim & Anderson, 2020a, 2020b) and submitted to a priori paired sample *t*-tests (two-tailed). Three paired sample *t*-tests were conducted on the peak beta weight estimates using the “-Clustsim” option under 3dttest++

(voxelwise $p < .005$, clusterwise $\alpha < .05$), a more conservative and nonparametric method for determining cluster-level threshold values (Cox et al., 2017). We compared trials where the target appeared in the previously high-value quadrant (valid) versus trials where the target appeared contralateral to the previously high-value quadrant (invalid), separately for each of the two hemifields (i.e., the peak of regressor 1 vs. 5 and 2 vs. 6) (as in Anderson et al., 2014; Anderson, 2017; Kim & Anderson, 2020a, 2020b). We focused on invalid trials in which the target was in the opposite hemifield as the previously reward-associated quadrant in order to isolate trials of maximal spatial competition between the target and reward history. The third paired sample *t*-test was conducted comparing no-target trials in which the previously reward-associated quadrant was on the left and right (i.e., the peak for regressor 7 vs. 8). A posthoc contrast using 3dANOVA3 was conducted to compare activations with respect to target hemifield (left vs right, collapsed across reward conditions). This contrast was corrected for multiple comparisons using the AFNI program 3dClustSim, with the smoothness of the data estimated using the ACF method (clusterwise $\alpha < .05$, voxelwise $p < .005$).

3 | RESULTS

3.1 | Behavior

During the training phase, participants were able to learn the reward association. The proportion of trials on which the high-value quadrant was selected in the final run was high (0.962; see Figure 2a) and averaged across all runs (0.784) was well above chance, $t(33)=19.35$, $p < .001$, $d=3.32$. Pairwise comparisons show that participants on average made more high-value choices on the last run compared to the first, $t(33)=15.1$, $p < .001$, $d=2.59$. During the test phase, accuracy was high (97.5%), and participants were faster to respond to valid trials compared to invalid trials, $t(33)=7.99$, $p < .001$, $d=1.37$

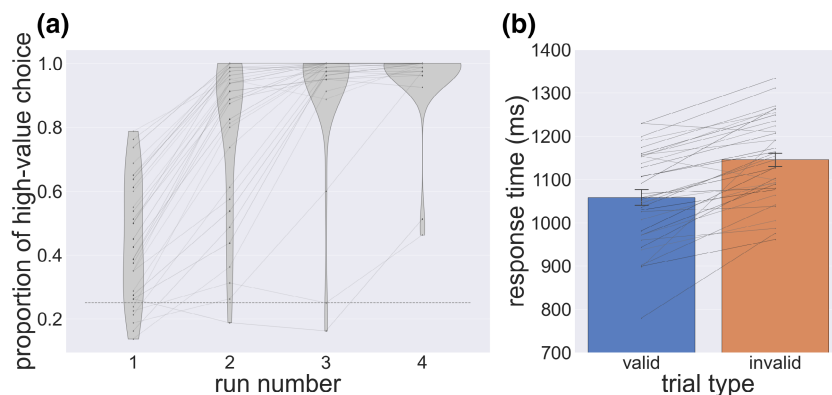


FIGURE 2 Behavioral results in the training and test phase. (a) Proportion of high-value choice by run during the training phase. (b) Response time in the test phase by trial type. Error bars reflect standard error of the means.

(see Figure 2b). For the 19 participants we had eye tracking data for, initial fixations over all trials were significantly biased toward the high-value quadrant (33.6%), $t(18)=7.68$, $p<.001$, $d=1.76$. On trials where the targets and distractors were presented, initial fixations were significantly biased toward the high-value quadrant (33.5%), $t=7.88$, $p<.001$, $d=1.81$, and toward the target quadrant (29.0%), $t(18)=2.70$, $p=.015$, $d=0.62$. On trials where the target and distractors were not presented, total fixation duration was higher on high-value quadrants (2992 ms) compared to low-value quadrants (2012 ms), $t(18)=4.33$, $p<.001$, $d=0.99$ and initial fixations were significantly biased toward the high-value quadrant (38.4%), $t(18)=3.84$, $p=.001$, $d=0.88$. The behavioral data on both target-present and no-target trials fully replicate Anderson and Kim (2018a, 2018b).

3.2 | Neuroimaging

We compared valid trials in which the target appears in the same quadrant that was previously associated with reward against invalid trials in which the previously reward-associated quadrant is in the opposite hemifield (see Figure 3). Valid trials evoked elevated responses in oculomotor areas of the value-driven attention network (Anderson, 2017, 2019; Kim & Anderson, 2020a, 2020b), including the caudate tail, superior colliculus, and frontal eye field. We also observed increased activation on valid trials in the medial temporal lobes, particularly in regions associated with scene, space, and object processing like the hippocampus (O'Keefe & Nadel, 1978), parahippocampal gyrus (Epstein & Kanwisher, 1998; Maguire et al., 1996), and the lateral occipital cortex (Grill-Spector et al., 2001).

These are not regions typically associated with the value-driven attention network but may have been recruited to represent additional reward-related information in object-rich scenes. We also observed an increase in activity for the insula and anterior cingulate cortex (ACC), which have been previously implicated in reward-modulated attentional control (Hickey et al., 2010; Wang et al., 2015).

Probing no-target trials where only the scenes were presented revealed no significant activations as a function of whether the previously reward-associated quadrant was on the left or right. To examine target-related activation, we compared activity on trials where the target appeared on the left versus the right hemifield (see Figure 4) and observed increased activity in the left extrastriate visual cortex and decreased activity in the right extrastriate visual cortex, indicating more elevated activation ipsilateral to the target. A complete list of all regions activated across all contrasts is provided in Table S2.

4 | DISCUSSION

In the present study, we investigated the neural basis of attentional priority for the region of a scene previously associated with reward. As in Anderson and Kim (2018a), we observed persistent spatial biases specific to different scenes in the form of cueing effects on RT and oculomotor biases; all behavioral measures indicated a persisting spatial bias toward previously high-reward locations in scenes. Our neuroimaging data comparing valid and invalid trials reveal some of the same neural correlates associated with value-driven feature-based attention, including the superior colliculus, frontal eye field, and caudate tail (Anderson, 2017;

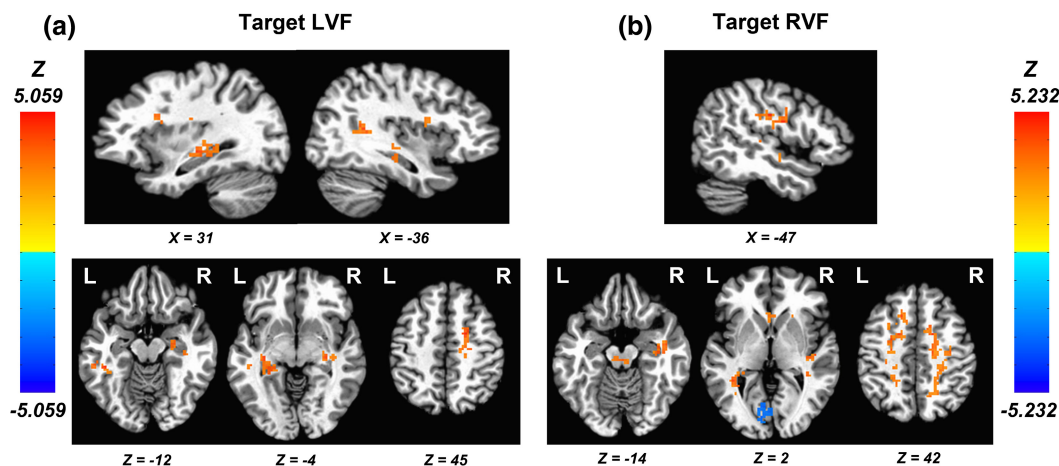


FIGURE 3 Regions in which activation differed between valid compared to invalid (high-value quadrant in opposite hemifield) trials during the test phase for targets appearing in the (a) left visual field (LVF) and (b) right visual field (RVF). The contrast is set up such that warmer colors indicate greater activation on value trials. Activations are overlaid on an image of the Talairach brain. A complete list of all regions showing significant activation is provided in Table S2.

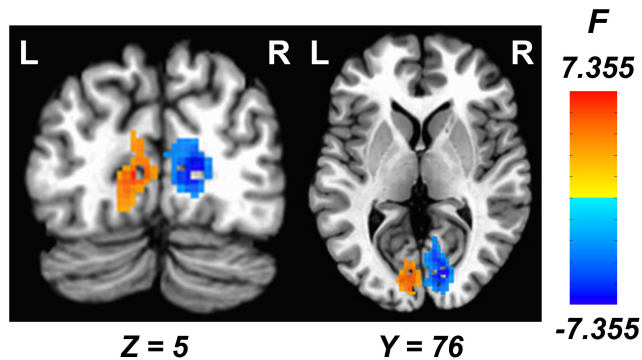


FIGURE 4 Regions that were significantly more active in response to the presentation of targets in the left vs right hemifield. The contrast depicted is the difference between left and right (left–right), such that cooler colors correspond to stronger activations in response to targets on the right and warmer colors to targets on the left.

Anderson et al., 2014, 2016, 2017; Bourgeois et al., 2022; Hickey & Peelen, 2015; Kim & Anderson, 2019b, 2020a, 2020b). We also observed such elevated stimulus-evoked activity in the insula and ACC, each of which has likewise been linked to value-driven feature-based orienting (Hickey et al., 2010; Wang et al., 2015). That is, targets evoked stronger activation in these regions when appearing in a previously reward-associated quadrant of the scene compared to when the previously reward-associated quadrant was in the opposite visual hemifield as the target, reflecting value-biased competition modulated by reward history tied to space.

In this experimental paradigm, we used object-rich scenes to provide contextual information about the location of high-value quadrants. Accordingly, we observed increased activation on valid trials—in which the task required the participant to orient to the previously high-value quadrant—in regions of the brain known to play an important role in representing spatial layout, including the hippocampus, parahippocampal gyrus, and occipitotemporal cortex (Epstein & Kanwisher, 1998; Maguire et al., 1996; O’keefe & Nadel, 1978). Such regions have not been previously implicated in value-driven attention and may be particular to reward’s modulatory influence on spatial orienting in scenes. It is possible that these regions only become preferentially activated after an orienting response has been made, reflecting biased competition from the scene as a function of reward history after the target quadrant has been selected.

The caudate tail, along with the superior colliculus and frontal eye field, have been frequently linked to value-driven attentional capture by feature-defined stimuli (Anderson, 2016). Given its connections with the superior colliculus (Yamamoto et al., 2012) and its proximity to the medial temporal lobe (Seger, 2013), the caudate tail potentially serves a more general role in value-based attentional

guidance by taking input from specific reward-associated features that are the targets of saccades as well as scene contexts associated with corresponding spatial priority. Such scene context representations may be mediated by the hippocampus, parahippocampal gyrus, and lateral occipital cortex (Epstein & Kanwisher, 1998; Maguire et al., 1996; O’keefe & Nadel, 1978). One of the most prominent spatial priority maps that guide attention is held in the posterior parietal cortex (Serences & Yantis, 2007; Sprague & Serences, 2013) and was not reliably activated in our task, in contrast to prior studies of feature-based value-driven attention (e.g., Anderson, 2017, 2019; Anderson et al., 2014; Kim & Anderson, 2020a, 2020b; see also Bourgeois et al., 2022). The lack of parietal cortex activity may reflect a distinction between the representation of feature-based and scene-based overt attention; the parietal cortex is situated closer to the occipital lobe and may be more suited for representing and prioritizing low-level features (Anderson, 2019; Serences & Yantis, 2007; Sprague & Serences, 2013), while information based on spatial context and layout is represented in the medial temporal lobe closer to the caudate tail (Epstein & Kanwisher, 1998; Maguire et al., 1996; O’keefe & Nadel, 1978). Future investigations should involve a closer look at time series data to determine the directionality and connectivity of these distinct brain regions, especially between regions known to represent value-driven attentional biases and those known to represent scene, space, and object identity.

Covert and overt attention often work in tandem to select relevant areas to fixate, since the fovea is where acuity is greatest. Although both pure spatial (covert) attention and eye movements (overt spatial attention) rely on a similar set of regions, such as those in the parietal and frontal lobes (Corbetta et al., 1998), frontal eye field (Bruce et al., 1985), and superior colliculus (Müller et al., 2005), their effects on perception are not always the same (Hunt & Kingstone, 2003a, 2003b; Kowler, 2011; Nakayama & Martini, 2011). Most notably, covert spatial attention can be applied to multiple regions in space simultaneously, whereas overt spatial attention can only be applied to a single location at once (Carrasco, 2011). The present study only measured spatial biases via overt eye movements, so the effect of reward learning on covert spatial attention remains unclear. However, given the overlap at both the neural (Bruce et al., 1985; Corbetta et al., 1998; Müller et al., 2005) and behavioral levels (Godijn & Theeuwes, 2002; Van der Stigchel & Theeuwes, 2005, 2007), our findings likely have some implications for mechanisms of value-driven covert spatial attention as well, although studies specifically isolating covert spatial attention are needed to explore where the underlying mechanisms overlap and where they might dissociate.

Our findings were in some respects similar to those of Bourgeois et al. (2022), particularly with regard to implicating the frontal eye field and superior colliculus, which provides converging evidence that value-biased competition for covert and overt attentional priority across features and space relies on similar anatomical regions. Interestingly, we also observed involvement from the hippocampus, parahippocampal gyrus, and occipitotemporal regions, which may be due to differences in the nature of the value-modulated representation we probed. Bourgeois et al. (2022) examined the spatial processing of a feature-defined cue using color-reward associations, while we focused more on the role of scenes as spatial contextual information where *locations themselves* are associated with reward. Anatomical regions processing scene, space, and objects may have been recruited to handle the increased richness of spatial information guiding attention. In this respect, our study provides unique insights into the neural mechanisms by which spatially-specific representations bound to different scenes are modulated by value and bias in visual information processing.

On free-viewing trials where only the scene is presented, there were longer dwell times on previously reward-associated quadrants, and these quadrants were more likely to be fixated first, replicating previous findings (Anderson & Kim, 2018a, 2018b). Such a bias in oculomotor behavior was not associated with significant modulations of neural activity. The inclusion of target-present trials, in which the high-value quadrant either competed with or complemented goal-directed spatial attentional processes, may have provided a more sensitive assessment of learning-dependent modulations of stimulus processing.

When examining target-evoked activation as a function of hemifield, greater activation ipsilateral to the target was observed collapsing across reward conditions. One possible explanation for this pattern of results is that participants were, to some degree, suppressing the background scene to better respond to the superimposed target. This interpretation is consistent with a prior finding where the multivoxel information content of objects in real-world scenes was suppressed for reward-associated distractors, and the strength of this suppression was associated with the degree of distractor-related impairment (Barbaro et al., 2017; Hickey & Peelen, 2015; Seidl et al., 2012; van Zoest et al., 2021; see also Payne et al., 2008).

Some studies using a single high-value location against a blank background have shown that learned spatial biases do not persist into extinction (Jiang et al., 2015; Won & Leber, 2016). Using scenes comprised of object-less textures, Anderson and Kim (2018b) found a reliable spatial bias evident during free viewing but not during performance of a visual search task as in the present study

(Anderson & Kim, 2018a). It is likely that the value-driven spatial biases observed in the present study require a distinct arrangement of objects within a scene, the spatial relationship among which serves as a contextual cue (Brockmole & Henderson, 2006a, 2006b). Accordingly, our observed neural correlates include visual regions traditionally associated with object processing like the lateral occipital cortex (Grill-Spector et al., 2001) and scene memory such as the temporo-occipital and parahippocampal cortex (Epstein & Kanwisher, 1998; Maguire et al., 1996).

The ACC is often associated with control processes like filtering, resolving of conflict, or gating of inputs (Mansouri et al., 2009), and is also thought to play a role in valuation signals that promote the repetition of a rewarded orienting response to a particular stimulus feature (reward-modulated priming; Hickey et al., 2010; see also Kaping et al., 2011). In the present study, valid trials, which preferentially activated the ACC, also involved the repetition of a previously rewarded orienting response, in this case with respect to a spatial context. In this respect, our findings are further consistent with a parallel influence of reward on feature-based and spatial attentional biases, and the recruitment of similar brain structures in spite of substantial differences between tasks.

In summary, our results suggest distinct neural correlates of value-driven spatial orienting in the hippocampus, parahippocampal gyrus, and surrounding cortices, as well as core regions of a value-driven attention network that are recruited in support of both feature-based and spatial (overt attentional) priority, including the caudate tail, superior colliculus, and frontal eye field. Given its role in the control of eye movements (Yamamoto et al., 2012, 2013) and proximity to both the hippocampus and parahippocampal gyrus on the one hand and its connections with the ventral visual stream on the other hand (Seger, 2013), the caudate tail may be particularly suited to serve as a hub region, playing a more central role in integrating value-based attentional priority across features and space, consistent with its central role in models of value-based attention (Anderson, 2019). We did not observe biased representation in the posterior parietal cortex, consistent with the dual mechanism of the value-driven attention hypothesis (Anderson, 2019) and a distinctly feature-based mode of priority in this case. Our task incorporated object-rich scenes into the signaling of value, with scene-space reward contingencies, which may have resulted in scene- and object-specific regions being recruited into the value-driven attention network, highlighting a greater flexibility in the neural computation of value-based attention priority than previously assumed (Anderson, 2019). The novel correlates of value-driven attention observed here provide an impetus for future research investigating the role of the medial temporal lobe in creating context-specific value-driven attentional biases (see, e.g., Anderson, 2015).

AUTHOR CONTRIBUTIONS

Ming-Ray Liao: Conceptualization; data curation; formal analysis; investigation; methodology; project administration; software; validation; visualization; writing – original draft; writing – review and editing. **Andy J. Kim:** Formal analysis; supervision; writing – original draft; writing – review and editing. **Brian A. Anderson:** Conceptualization; funding acquisition; resources; supervision; writing – original draft; writing – review and editing.

ACKNOWLEDGMENTS

We thank Mark K. Britton for assistance with data collection.

FUNDING INFORMATION

This research was supported by a start-up package from Texas A&M University to BAA and grants from the Brain & Behavior Research Foundation [NARSAD 26008] and NIH [R01-DA406410] to BAA.

CONFLICT OF INTEREST STATEMENT

The authors declare no conflicts of interest.

DATA AVAILABILITY STATEMENT

Deidentified raw behavioral and fMRI data, as well as analyses scripts for the experiment will be made available in a publicly accessible repository upon notification of acceptance of the manuscript.

ORCID

Ming-Ray Liao  <https://orcid.org/0000-0001-7418-9625>

REFERENCES

- Anderson, B. A. (2015). Value-driven attentional priority is context specific. *Psychonomic Bulletin & Review*, 22(3), 750–756. <https://doi.org/10.3758/s13423-014-0724-0>
- Anderson, B. A. (2016). The attention habit: How reward learning shapes attentional selection. *Annals of the New York Academy of Sciences*, 1369(1), 24–39. <https://doi.org/10.1111/nyas.12957>
- Anderson, B. A. (2017). Reward processing in the value-driven attention network: Reward signals tracking cue identity and location. *Social Cognitive and Affective Neuroscience*, 12(3), 461–467. <https://doi.org/10.1093/scan/nsw141>
- Anderson, B. A. (2019). Neurobiology of value-driven attention. *Current Opinion in Psychology*, 29, 27–33. <https://doi.org/10.1016/j.copsyc.2018.11.004>
- Anderson, B. A., & Britton, M. K. (2019). On the automaticity of attentional orienting to threatening stimuli. *Emotion*, 20, 1109–1112. <https://doi.org/10.1037/emo0000596>
- Anderson, B. A., & Kim, H. (2018a). Mechanisms of value-learning in the guidance of spatial attention. *Cognition*, 178, 26–36. <https://doi.org/10.1016/j.cognition.2018.05.005>
- Anderson, B. A., & Kim, H. (2018b). On the representational nature of value-driven spatial attentional biases. *Journal of Neurophysiology*, 120(5), 2654–2658. <https://doi.org/10.1152/jn.00489.2018>
- Anderson, B. A., & Kim, H. (2019a). On the relationship between value-driven and stimulus-driven attentional capture. *Attention, Perception, and Psychophysics*, 81, 607–613. <https://doi.org/10.3758/s13414-019-01670-2>
- Anderson, B. A., & Kim, H. (2019b). Test-retest reliability of value-driven attentional capture. *Behavior Research Methods*, 51, 720–726. <https://doi.org/10.3758/s13428-018-1079-7>
- Anderson, B. A., Kuwabara, H., Wong, D. F., Gean, E. G., Rahmim, A., Brašić, J. R., George, N., Frolov, B., Courtney, S. M., & Yantis, S. (2016). The role of dopamine in value-based attentional orienting. *Current Biology*, 26(4), 550–555. <https://doi.org/10.1016/j.cub.2015.12.062>
- Anderson, B. A., Kuwabara, H., Wong, D. F., Roberts, J., Rahmim, A., Brašić, J. R., & Courtney, S. M. (2017). Linking dopaminergic reward signals to the development of attentional bias: A positron emission tomographic study. *NeuroImage*, 157, 27–33. <https://doi.org/10.1016/j.neuroimage.2017.05.062>
- Anderson, B. A., Laurent, P. A., & Yantis, S. (2011). Value-driven attentional capture. *Proceedings of the National Academy of Sciences*, 108(25), 10367–10371. <https://doi.org/10.1073/pnas.1104047108>
- Anderson, B. A., Laurent, P. A., & Yantis, S. (2014). Value-driven attentional priority signals in human basal ganglia and visual cortex. *Brain Research*, 1587, 88–96. <https://doi.org/10.1016/j.brainres.2014.08.062>
- Anderson, B. A., & Yantis, S. (2012). Value-driven attentional and oculomotor capture during goal-directed, unconstrained viewing. *Attention, Perception, and Psychophysics*, 74, 1644–1653. <https://doi.org/10.3758/s13414-012-0348-2>
- Anderson, B. A., & Yantis, S. (2013). Persistence of value-driven attentional capture. *Journal of Experimental Psychology: Human Perception and Performance*, 39(1), 6–9. <https://doi.org/10.1037/a0030860>
- Barbaro, L., Peelen, M. V., & Hickey, C. (2017). Valence, not utility, underlies reward-driven prioritization in human vision. *Journal of Neuroscience*, 37, 10438–10450. <https://doi.org/10.1523/JNEUROSCI.1128-17.2017>
- Bourgeois, A., Sterpenich, V., Iannotti, G. R., & Vuilleumier, P. (2022). Reward-driven modulation of spatial attention in the human frontal eye-field. *Neuroimage*, 247, 118846. <https://doi.org/10.1016/j.neuroimage.2021.118846>
- Brainard, D. H. (1997). The psychophysics toolbox. *Spatial Vision*, 10(4), 433–436. <https://doi.org/10.1163/156856897X00357>
- Britton, M. K., & Anderson, B. A. (2020). Specificity and persistence of statistical learning in distractor suppression. *Journal of Experimental Psychology: Human Perception and Performance*, 46(3), 324–334. <https://doi.org/10.1037/xhp0000718>
- Brockmole, J. R., & Henderson, J. M. (2006a). Recognition and attention guidance during contextual cueing in real-world scenes: Evidence from eye movements. *Quarterly Journal of Experimental Psychology (Hove)*, 59, 1177–1187. <https://doi.org/10.1080/17470210600665996>
- Brockmole, J. R., & Henderson, J. M. (2006b). Using real-world scenes as contextual cues for search. *Visual Cognition*, 13, 99–108. <https://doi.org/10.1080/13506280500165188>
- Bruce, C. J., Goldberg, M. E., Bushnell, M. C., & Stanton, G. B. (1985). Primate frontal eye fields: II. Physiological and anatomical correlates of electrically evoked eye movements. *Journal*

- of *Neurophysiology*, 54, 714–734. <https://doi.org/10.1152/jn.1985.54.3.714>
- Carrasco, M. (2011). Visual attention: The past 25 years. *Vision Research*, 51(13), 1484–1525. <https://doi.org/10.1016/j.visres.2011.04.012>
- Chelazzi, L., Estocinova, J., Calletti, R., Lo Gerfo, E., Sani, I., Della Libera, C., & Santandrea, E. (2014). Altering spatial priority maps via reward-based learning. *Journal of Neuroscience*, 34, 8594–8604. <https://doi.org/10.1523/JNEUROSCI.0277-14.2014>
- Corbetta, M., Akbudak, E., Conturo, T. E., Snyder, A. Z., Ollinger, J. M., Drury, H. A., Linenweber, M. R., Petersen, S. E., Raichle, M. E., van Essen, D. C., & Shulman, G. L. (1998). A common network of functional areas for attention and eye movements. *Neuron*, 21, 761–773. [https://doi.org/10.1016/S0896-6273\(00\)80593-0](https://doi.org/10.1016/S0896-6273(00)80593-0)
- Cox, R. W. (1996). AFNI: Software for analysis and visualization of functional magnetic resonance neuroimages. *Computers and Biomedical Research*, 29(3), 162–173. <https://doi.org/10.1006/cbmr.1996.0014>
- Cox, R. W., Chen, G., Glen, D. R., Reynolds, R. C., & Taylor, P. A. (2017). FMRI clustering in AFNI: False-positive rates redux. *Brain Connectivity*, 7(3), 152–171. <https://doi.org/10.1089/brain.2016.0475>
- Della Libera, C., & Chelazzi, L. (2009). Learning to attend and to ignore is a matter of gains and losses. *Psychological Science*, 20(6), 778–784. <https://doi.org/10.1111/j.1467-9280.2009.02360.x>
- Della Libera, C., Perlato, A., & Chelazzi, L. (2011). Dissociable effects of reward on attentional learning: From passive associations to active monitoring. *PLoS One*, 6(4), e19460. <https://doi.org/10.1371/journal.pone.0019460>
- Desimone, R., & Duncan, J. (1995). Neural mechanisms of selective visual attention. *Annual Review of Neuroscience*, 18(1), 193–222. <https://doi.org/10.1146/annurev.ne.18.030195.001205>
- Donohue, S. E., Hopf, J.-M., Bartsch, M. V., Schoenfeld, M. A., Heinze, H.-J., & Woldorff, M. G. (2016). The rapid capture of attention by rewarded objects. *Journal of Cognitive Neuroscience*, 28(4), 529–541. https://doi.org/10.1162/jocn_a_00917
- Epstein, R., & Kanwisher, N. (1998). A cortical representation of the local visual environment. *Nature*, 392(6676), 598–601. <https://doi.org/10.1038/33402>
- Folk, C. L., Remington, R. W., & Johnston, J. C. (1992). Involuntary covert orienting is contingent on attentional control settings. *Journal of Experimental Psychology: Human Perception and Performance*, 18(4), 1030–1044. <https://doi.org/10.1037/0096-1523.18.4.1030>
- Godijn, R., & Theeuwes, J. (2002). Programming of endogenous and exogenous saccades: Evidence for a competitive integration model. *Journal of Experimental Psychology: Human Perception & Performance*, 28, 1039–1054. <https://doi.org/10.1037/0096-1523.28.5.1039>
- Grégoire, L., Kim, H., & Anderson, B. A. (2021). Punishment-modulated attentional capture is context specific. *Motivation Science*, 7, 165–175. <https://doi.org/10.1037/mot0000211>
- Grill-Spector, K., Kourtzi, Z., & Kanwisher, N. (2001). The lateral occipital complex and its role in object recognition. *Vision Research*, 41(10–11), 1409–1422. [https://doi.org/10.1016/S0042-6989\(01\)00073-6](https://doi.org/10.1016/S0042-6989(01)00073-6)
- Hickey, C., Chelazzi, L., & Theeuwes, J. (2010). Reward changes salience in human vision via the anterior cingulate. *Journal of Neuroscience*, 30(33), 11096–11103. <https://doi.org/10.1523/JNEUROSCI.1026-10.2010>
- Hickey, C., Kaiser, D., & Peelen, M. V. (2015). Reward guides attention to object categories in real-world scenes. *Journal of Experimental Psychology: General*, 144(2), 264–273. <https://doi.org/10.1037/a0038627>
- Hickey, C., & Peelen, M. V. (2015). Neural mechanisms of incentive salience in naturalistic human vision. *Neuron*, 85(3), 512–518. <https://doi.org/10.1016/j.neuron.2014.12.049>
- Hickey, C., & Peelen, M. V. (2017). Reward selectively modulates the lingering neural representation of recently attended objects in natural scenes. *Journal of Neuroscience*, 37, 7297–7304. <https://doi.org/10.1523/JNEUROSCI.0684-17.2017>
- Hunt, A. R., & Kingstone, A. (2003a). Covert and overt voluntary attention: Linked or independent? *Cognitive Brain Research*, 18, 102–105. <https://doi.org/10.1016/j.cogbr.ainres.2003.08.006>
- Hunt, A. R., & Kingstone, A. (2003b). Inhibition of return: Dissociating attentional and oculomotor components. *Journal of Experimental Psychology: Human Perception & Performance*, 29, 1068–1074. <https://doi.org/10.1037/0096-1523.29.5.1068>
- Ikeda, T., & Hikosaka, O. (2003). Reward-dependent gain and bias of visual responses in primate superior colliculus. *Neuron*, 39(4), 693–700. [https://doi.org/10.1016/S0896-6273\(03\)00464-1](https://doi.org/10.1016/S0896-6273(03)00464-1)
- Itthipuripat, S., Vo, V. A., Sprague, T. C., & Serences, J. T. (2019). Value-driven attentional capture enhances distractor representations in early visual cortex. *PLoS Biology*, 17, e3000186. <https://doi.org/10.1371/journal.pbio.3000186>
- Jiang, Y. V., Sha, L. Z., & Remington, R. W. (2015). Modulation of spatial attention by goals, statistical learning, and monetary reward. *Attention, Perception, & Psychophysics*, 77(7), 2189–2206. <https://doi.org/10.3758/s13414-015-0952-z>
- Kaping, D., Vinck, M., Hutchison, R. M., Everling, S., & Womelsdorf, T. (2011). Specific contributions of ventromedial, anterior cingulate, and lateral prefrontal cortex for attentional selection and stimulus valuation. *PLoS Biology*, 9(12), e1001224. <https://doi.org/10.1371/journal.pbio.1001224>
- Kim, A. J., & Anderson, B. A. (2020a). Arousal-biased competition explains reduced distraction by reward cues under threat. *eNeuro*, 7(4), ENEURO.0099-20.2020. <https://doi.org/10.1523/ENEURO.0099-20.2020>
- Kim, A. J., & Anderson, B. A. (2020b). Neural correlates of attentional capture by stimuli previously associated with social reward. *Cognitive Neuroscience*, 11(1–2), 5–15. <https://doi.org/10.1080/17588928.2019.1585338>
- Kim, H., & Anderson, B. A. (2019a). Dissociable components of experience-driven attention. *Current Biology*, 29, 841–845. <https://doi.org/10.1016/j.cub.2019.01.030>
- Kim, H., & Anderson, B. A. (2019b). Dissociable neural mechanisms underlie value-driven and selection-driven attentional capture. *Brain Research*, 1708, 109–115. <https://doi.org/10.1016/j.brainres.2018.11.026>
- Kim, H., & Anderson, B. A. (2019c). Neural evidence for automatic value-modulated approach behaviour. *NeuroImage*, 189, 150–158. <https://doi.org/10.1016/j.neuroimage.2018.11.026>
- Kim, H. F., & Hikosaka, O. (2013). Distinct basal ganglia circuits controlling behaviors guided by flexible and stable values. *Neuron*, 79(5), 1001–1010. <https://doi.org/10.1016/j.neuron.2013.06.044>
- Kowler, E. (2011). Eye movements: The past 25 years. *Vision Research*, 51(13), 1457–1483. <https://doi.org/10.1016/j.visres.2010.12.014>

- Laurent, P. A., Hall, M. G., Anderson, B. A., & Yantis, S. (2015). Valuable orientations capture attention. *Visual Cognition*, 23(1-2), 133–146. <https://doi.org/10.1080/13506285.2014.965242>
- Le Pelley, M. E., Pearson, D., Griffiths, O., & Beesley, T. (2015). When goals conflict with values: Counterproductive attentional and oculomotor capture by reward-related stimuli. *Journal of Experimental Psychology: General*, 144, 158–171. <https://doi.org/10.1037/xge0000037>
- Lee, J., & Shomstein, S. (2014). Reward-based transfer from bottom-up to top-down search tasks. *Psychological Science*, 25(2), 466–475. <https://doi.org/10.1177/0956797613509284>
- Liao, M. R., & Anderson, B. A. (2020a). Inertia in value-driven attention. *Learning & Memory*, 27(12), 488–492. <https://doi.org/10.1101/lm.052027.120>
- Liao, M. R., & Anderson, B. A. (2020b). Reward learning biases the direction of saccades. *Cognition*, 196, 104145. <https://doi.org/10.1016/j.cognition.2019.104145>
- Liao, M. R., Britton, M. K., & Anderson, B. A. (2020). Selection history is relative. *Vision Research*, 175, 23–31. <https://doi.org/10.1016/j.visres.2020.06.004>
- MacLean, M. H., & Giesbrecht, B. (2015). Neural evidence reveals the rapid effects of reward history on selective attention. *Brain Research*, 1606, 86–94. <https://doi.org/10.1016/j.brainres.2015.02.016>
- Maguire, E. A., Frackowiak, R. S., & Frith, C. D. (1996). Learning to find your way: A role for the human hippocampal formation. *Proceedings of the Royal Society of London. Series B: Biological Sciences*, 263(1377), 1745–1750. <https://doi.org/10.1098/rspb.1996.0255>
- Mansouri, F. A., Tanaka, K., & Buckley, M. J. (2009). Conflict-induced behavioural adjustment: A clue to the executive functions of the prefrontal cortex. *Nature Reviews Neuroscience*, 10(2), 141–152. <https://doi.org/10.1038/nrn2538>
- Milner, A. E., MacLean, M. H., & Giesbrecht, B. (2023). The persistence of value-driven attention capture is task-dependent. *Attention, Perception, & Psychophysics*, 85, 315–341. <https://doi.org/10.3758/s13414-022-02621-0>
- Müller, J. R., Philiastides, M. G., & Newsome, W. T. (2005). Microstimulation of the superior colliculus focuses attention without moving the eyes. *Proceedings of the National Academy of Sciences*, 102, 524–529. <https://doi.org/10.1073/pnas.0408311101>
- Nakayama, K., & Martini, P. (2011). Situating visual search. *Vision Research*, 51(13), 1526–1537. <https://doi.org/10.1016/j.visres.2010.09.003>
- Nissens, T., Failing, M., & Theeuwes, J. (2017). People look at the object they fear: Oculomotor capture by stimuli that signal threat. *Cognition and Emotion*, 31(8), 1707–1714. <https://doi.org/10.1080/02699931.2016.1248905>
- O'Keefe, J., & Nadel, L. (1978). *The hippocampus as a cognitive map*. Clarendon Press.
- Payne, J. D., Stickgold, R., Swanberg, K., & Kensinger, E. A. (2008). Sleep preferentially enhances memory for emotional components of scenes. *Psychological Science*, 19(8), 781–788. <https://doi.org/10.1111/j.1467-9280.2008.02157.x>
- Sareen, P., Ehinger, K. A., & Wolfe, J. M. (2016). CB database: A change blindness database for objects in natural indoor scenes. *Behavior Research Methods*, 48(4), 1343–1348. <https://doi.org/10.3758/s13428-015-0640-x>
- Schmidt, L. J., Belopolsky, A. V., & Theeuwes, J. (2015). Attentional capture by signals of threat. *Cognition and Emotion*, 29(4), 687–694. <https://doi.org/10.1080/02699931.2014.924484>
- Seger, C. A. (2013). The visual corticostriatal loop through the tail of the caudate: Circuitry and function. *Frontiers in Systems Neuroscience*, 7, 104. <https://doi.org/10.3389/fnsys.2013.00104>
- Seidl, K. N., Peelen, M. V., & Kastner, S. (2012). Neural evidence for distracter suppression during visual search in real-world scenes. *Journal of Neuroscience*, 32(34), 11812–11819. <https://doi.org/10.1523/JNEUROSCI.1693-12.2012>
- Serences, J. T. (2008). Value-based modulations in human visual cortex. *Neuron*, 60(6), 1169–1181. <https://doi.org/10.1016/j.neuron.2008.10.051>
- Serences, J. T., & Saproo, S. (2010). Population response profiles in early visual cortex are biased in favor of more valuable stimuli. *Journal of Neurophysiology*, 104(1), 76–87. <https://doi.org/10.1152/jn.01090.2009>
- Serences, J. T., & Yantis, S. (2007). Spatially selective representations of voluntary and stimulus-driven attentional priority in human occipital, parietal, and frontal cortex. *Cerebral Cortex*, 17(2), 284–293. <https://doi.org/10.1093/cercor/bhj146>
- Sommer, M. A., & Wurtz, R. H. (2004). What the brain stem tells the frontal cortex. I. Oculomotor signals sent from superior colliculus to frontal eye field via mediodorsal thalamus. *Journal of Neurophysiology*, 91(3), 1381–1402. <https://doi.org/10.1152/jn.00738.2003>
- Sprague, T. C., & Serences, J. T. (2013). Attention modulates spatial priority maps in the human occipital, parietal and frontal cortices. *Nature Neuroscience*, 16(12), 1879–1887. <https://doi.org/10.1038/nn.3574>
- Talairach, J., & Tournoux, P. (1988). *Co-planar stereotaxic atlas of the human brain: 3-dimensional proportional system: An approach to cerebral imaging*. Georg Thieme.
- Theeuwes, J. (1992). Perceptual selectivity for color and form. *Perception & Psychophysics*, 51(6), 599–606. <https://doi.org/10.3758/BF03211656>
- Van der Stigchel, S., & Theeuwes, J. (2005). Relation between saccade trajectories and spatial distractor locations. *Cognitive Brain Research*, 25, 579–582. <https://doi.org/10.1016/j.cogbr.ainres.2005.08.001>
- Van der Stigchel, S., & Theeuwes, J. (2007). The relationship between covert and overt attention in endogenous cuing. *Perception & Psychophysics*, 69(5), 719–731. <https://doi.org/10.3758/bf03193774>
- van Zoest, W., Huber-Huber, C., Weaver, M. D., & Hickey, C. (2021). Strategic distractor suppression improves selective control in human vision. *Journal of Neuroscience*, 41(33), 7120–7135. <https://doi.org/10.1523/JNEUROSCI.0553-21.2021>
- Wang, B., & Theeuwes, J. (2018a). How to inhibit a distractor location? Statistical learning versus active, top-down suppression. *Attention, Perception, & Psychophysics*, 80, 860–870. <https://doi.org/10.3758/s13414-018-1493-z>
- Wang, B., & Theeuwes, J. (2018b). Statistical regularities modulate attentional capture. *Journal of Experimental Psychology: Human Perception and Performance*, 44, 13–17. <https://doi.org/10.1037/xhp0000472>
- Wang, B., & Theeuwes, J. (2018c). Statistical regularities modulate attentional capture independent of search strategy. *Attention, Perception, & Psychophysics*, 80, 1763–1774. <https://doi.org/10.3758/s13414-018-1562-3>

- Wang, L., Yu, H., Hu, J., Theeuwes, J., Gong, X., Xiang, Y., Jiang, C., & Zhou, X. (2015). Reward breaks through center-surround inhibition via anterior insula. *Human Brain Mapping, 36*(12), 5233–5251. <https://doi.org/10.1002/hbm.23004>
- Waskom, M. L. (2021). Seaborn: Statistical data visualization. *Journal of Open Source Software, 6*(60), 3021. <https://doi.org/10.21105/joss.03021>
- Wolfe, J. M., Cave, K. R., & Franzel, S. L. (1989). Guided search: An alternative to the feature integration model for visual search. *Journal of Experimental Psychology: Human Perception and Performance, 15*(3), 419–433. <https://doi.org/10.1037/0096-1523.15.3.419>
- Won, B. Y., & Leber, A. B. (2016). How do magnitude and frequency of monetary reward guide visual search. *Attention, Perception, & Psychophysics, 78*(5), 1221–1231. <https://doi.org/10.3758/s13414-016-1154-z>
- Yamamoto, S., Kim, H. F., & Hikosaka, O. (2013). Reward value-contingent changes of visual responses in the primate caudate tail associated with a visuomotor skill. *Journal of Neuroscience, 33*(27), 11227–11238. <https://doi.org/10.1523/JNEUROSCI.0318-13.2013>
- Yamamoto, S., Monosov, I. E., Yasuda, M., & Hikosaka, O. (2012). What and where information in the caudate tail guides saccades to visual objects. *Journal of Neuroscience, 32*(32), 11005–11016. <https://doi.org/10.1523/JNEUROSCI.0828-12.2012>

SUPPORTING INFORMATION

Additional supporting information can be found online in the Supporting Information section at the end of this article.

Supplemental Figure 1. Proportion of high-value choice by run during the training phase for the 34 participants that were eligible to continue the study in blue, and the eight participants in red that failed to robustly learn the scene-reward associations.

Table S1.

Table S2.

How to cite this article: Liao, M.-R., Kim, A. J., & Anderson, B. A. (2023). Neural correlates of value-driven spatial orienting. *Psychophysiology, 00*, e14321. <https://doi.org/10.1111/psyp.14321>